Supporting Information

A chemical-genetic approach to study G protein regulation of β cell function *in vivo*

Guettier et al.

SI Text

SI Materials and Methods

Generation of CNO-Sensitive Mutant M3Rs With Distinct G Protein Coupling Profiles. We recently described the generation of a mammalian expression plasmid (pBA-136) coding for a modified version of the human M3R containing the Y149C and A239G point mutations (1). Importantly, this mutant receptor did no longer respond to ACh, the endogenous M3R ligand, but could be activated by the otherwise pharmacologically inert drug, CNO, leading to the selective activation of $G_{q/11}$ (1). To introduce these two mutations into the rat M3R containing an N-terminal hemagglutinin (HA) epitope tag, we subcloned a 924 bp BstEII-SbfI fragment derived from pBA-136 into the corresponding sites of the mammalian expression plasmid, Rm3pcD-N-HA (2). For the sake of simplicity, we refer to this vector as R-q-pcD throughout the manuscript.

To generate a CNO-sensitive G_s-coupled mutant M3R that is unable to bind ACh, we first replaced the second and third intracellular loops (i2 and i3 loop, respectively) of the rat M3R with the corresponding turkey β_1-adrenergic receptor (β1AR) sequences (3). Specifically, in this hybrid receptor, the rat M3R i2 and i3 loops (sequences ^{171}RPLTYRAKRTTK^{182} and ^{253}IYKETEKRTK--220 aa--KEKKAA^{489}, respectively) were replaced with the corresponding turkey β1AR sequences (^{145}SPFRYQSLMTRA^{156} and ^{230}VYREAK--46 aa--MREHKAL^{289}, respectively). The turkey β1AR sequences were introduced into the Rm3pcD-N-HA vector by using standard recombinant PCR mutagenesis techniques. The Y148C and A238G point mutations were then substituted

into this hybrid construct via site-directed mutagenesis (QuikChange Invitrogen, Carlsbad, CA). These two point mutations correspond to the Y149C and A239G substitutions in the human M3R (1). For the sake of simplicity, we refer to the resulting plasmid as R-s-pcD throughout the manuscript.

Calcium Assays. We used FLIPR technology (Molecular Devices, Sunnyvale, CA) to measure receptor-mediated increases in intracellular calcium levels in transiently transfected COS-7 cells. About 24 hr after transfection, receptor-expressing COS-7 cells were seeded into 96-wells plate at a density of 2 x 10^5 cells/well. On the following day, cells were incubated for 1 h at 37 °C with 30 μl of loading dye (FLIPR Calcium 3 Assay Kit, Molecular Devices), supplemented with 5 mM probenecid to increase dye retention. Cells were then treated with increasing concentrations (10 pM to 1 mM) of ACh or CNO dissolved in HEPES-buffered (20 mM) Hanks' balanced salt solution (HBSS). Changes in cell fluorescence were measured at room temperature using a FLIPR^{TETRA} plate reader (Molecular Devices; excitation wavelength: 470-495 nm; emission wavelength: 515-575 nm). For each ligand concentration, increases in intracellular calcium levels were measured as peak fluorescence activity (FI) minus basal FI prior to the addition of ligand. Ligand concentration-response curves were analyzed by using GraphPad Prism 4.0 (GraphPad Software, La Jolla, CA). Assays were carried out in quadruplicate.

Generation of Transgenic Mice Selectively Expressing the R-q and R-s Designer Receptors in Pancreatic β Cells. To obtain transgenic mice selectively expressing the R-q and R-s mutant receptors in pancreatic β cells, two different transgenes were created in which the expression of the two receptors was placed under the transcriptional control of a 650 bp fragment of the rat insulin promoter II (RIPII; ref. 4). In order to generate the RIPII-R-q transgene, a 927 bp BstEII-AarI fragment from the R-q-pcD vector was ligated into the corresponding sites of the previously published RIP-M_3 transgene vector (5). A 4.6 kb EcoRV-EagI fragment containing the RIPII promoter, the entire R-q coding sequence, and 3' untranslated human growth hormone sequences (including transcriptional termination, polyadenylation, and splicing signals) was excised from RIPII-R-q, purified, and microinjected into the pronuclei of ova from fertilized C57BL/6NTac mice. The

RIPII-R-s transgene vector was created in a similar fashion by ligating a 720 bp BstEII-NheI fragment derived from R-s-pcD into the corresponding sites of the RIPII-R-q plasmid. A KpnI-NotI 4.2 kb transgene fragment containing the entire R-s coding sequence was removed from RIPII-R-s, purified, and microinjected into the pronuclei of ova from fertilized C57BL/6NTac mice. Following this protocol, we identified several founder mice for each of the two transgene constructs that stably transmitted the transgene to their progeny. For the present study, we amplified two independent transgenic mouse lines, referred to as β-R-q Tg and β-R-s Tg mice. These lines were chosen because they expressed comparable levels of mutant receptors in their pancreatic islets. Both lines were maintained on a pure C57BL/6NTac background.

Mouse Genotyping Studies. The presence of the RIPII-R-q and RIPII-R-s transgene in mouse tail genomic DNA was detected by PCR. In the case of RIPII-R-q, a 303 bp PCR product was amplified using the following transgene-specific primers: 5'-CCCTACGACGTCCCCGACTACG (forward), 5'-GACCTTAAATGACCAATTACCA (reverse). In the case of RIPII-R-s, a 308 bp PCR product was generated using the following transgene-specific primer pair: 5'-GAGCCTGATGACCAGGGCT (forward), 5'-GCGGCTGCTCCTGGCTGCCATA (reverse). The following PCR cycling conditions were used: 94 °C for 10 min, followed by 28 cycles at 94 °C for 30 s, 56 °C for 30 s, and 72 °C for 30 s.

RT-PCR Analysis of Transgene Expression. Total RNA was extracted from various peripheral and central tissues of β-R-q and β-R-s Tg mice using the QIAzol Lysis Reagent (Qiagen, Valencia, CA). During this procedure, an on-column DNase I treatment step was performed (RNeasy Mini Kit; Qiagen). Total RNA (50 ng per sample) was reverse transcribed into cDNA using the Superscript™ III first-strand synthesis kit (Invitrogen, Carlsbad, CA). R-q and R-s-specific PCR primer pairs were used for PCR reactions (for primer sequences, see 'Mouse genotyping studies'). Each PCR reaction contained 5 ng cDNA, 0.5 μl AmpliTaq Gold (Applied Biosystems, Foster City, CA), 250 μM of each dNTP (Applied Biosystems), 4 μl 10 x PCR buffer containing 15 mM $MgCl_2$, 0.5 μM of each PCR primer, and was adjusted to a final volume of 40 μl with water. The following

PCR cycling conditions were used: 94 °C for 10 min, followed by 28 cycles at 94 °C for 30 s, 56 °C for 30 s, and 72 °C for 30 s.

Morphometric Analysis of Pancreatic Islets. Islet morphometric studies were performed using 8-week-old female mice (three mice per strain and treatment group). Mice were injected daily with either saline or CNO (1 mg/kg i.p.) for a 2-week period. At the end of the injection period, pancreata were rapidly isolated, fixed in 10% neutral buffered formalin overnight, and embedded in paraffin. For each pancreas, 5 μm-thick sections from five distinct levels, 200 μm apart, were mounted on slides and stained for insulin and terminal dUTP nick-end labeling (TUNEL). β-cell cells were identified by immunostaining for insulin using an guinea-pig anti-insulin antibody (dilution 1:500; Dako). Apoptotic cells were identified by TUNEL staining using the ApopTag Peroxidase In Situ Apoptosis kit (Chemicon/Millipore, Temecula, CA). An ABC kit using 3,3'-diaminobenzidine chemistry (Vectastain, Burlingame, CA) was used for the detection of primary antibodies. All sections were lightly counterstained with hematoxylin.

To determine β cell mass, five pancreatic sections per animal (200 μm apart) were photographed at 50 x magnification using an Axiocam MRm digital camera mounted on a Zeiss Axiovert Imager D1 imaging system (Zeiss, Thornwood, NY). Image acquisition and measurements of total pancreatic and β cell-specific (insulin-stained) area for each section were obtained using AxioVision software 4.5 (Zeiss, Thornwood, NY). The ratio of islet cross-sectional area to total pancreatic area was multiplied by pancreatic weight to obtain β cell mass.

Following TUNEL staining, islets were photographed (at 50 x) and analyzed using the same software as described above. The ratio of stained islet nuclei to the total number of islet nuclei was determined. Mean β cell (islet cell) size was assessed by dividing islet cross-sectional area by the number of islet nuclei. At least 2,500 cells were counted from 4 sections (200 μm apart) of each pancreas.

Real-Time qRT-PCR Analysis of Islet Gene Expression. Pancreatic islets were prepared from β-R-q and β-R-s Tg mice and WT littermates as described above (3-4 mice per strain per experiment). For real-time qRT-PCR experiments, freshly prepared islets

(>100 islets/sample) were cultured in a 5 % CO_2 incubator at 37 °C for 3 hr in RPMI 1640 cell culture medium (Invitrogen, Carlsbad, CA) supplemented with 5.5 mM glucose, 10% fetal bovine serum, 100 U/ml penicillin, and 100 μg/ml streptomycin. Islets were cultured either in the presence or in the absence of 1 μM CNO. Subsequently, total islet RNA was isolated and purified using RNeasy columns, including an on column DNAse I treatment step (Qiagen, Valencia, CA.) Total RNA (100 ng per sample) was reverse transcribed into cDNA using the Superscript™ III first-strand synthesis kit (Invitrogen, Carlsbad, CA). Gene expression was determined by monitoring SYBR green fluorescence intensity over time using an ABI 7900HT Fast Real-Time PCR System (Applied Biosystems). Each PCR reaction (final volume: 20 μl) consisted of cDNA (~5 ng), 10 μl of SYBR Green PCR master mix (Applied Biosystems), and 150 nM of each PCR primer. For each primer pair, qRT-PCR reactions were performed in triplicate using a 96-well plate format. Specificity of each primer pair was confirmed by melting curve analysis. Primers were selected from previously validated primer sets obtained from the Harvard Primer Bank (6). PCR cycling conditions were as follows: 50 °C for 2 min, 95 °C for 10 min, and 40 cycles at 95 °C for 15 s, and 60 °C for 1 min respectively. The expression of cyclophilin A served as an internal control. The ΔΔCt method was used to compare fold changes in mRNA expression between control and CNO-treated mice (for primer sequences, see Table S2).

Analysis of CNO and Clozapine Plasma Levels. To rule out the possibility that CNO was metabolically converted to its parent compound, clozapine, i*n vivo*, WT C57BL/6NTac mice (3-month-old females; n = 3) received a single injection of CNO (1 mg/kg i.p.). Blood samples (30-50 μl) were collected from the retro-orbital sinus immediately prior to and 15, 30 and 60 min following CNO injection. Plasma CNO and clozapine concentrations were determined by liquid chromatography tandem mass spectrometry (LC-MS/MS). Briefly, LC-MS/MS analysis was performed using an API 2000 ESI triple quadrupole mass spectrometer (Applied Biosystems). A Luna 3 mm 50 x 4.6 mm C18 column (Phenomenex, Torrance, CA) was used to separate CNO and clozapine. The flow rate through the column at ambient temperature was 0.25 ml/min using 70% aqueous methanol containing 0.1% formic acid. The mass spectrometer was

equipped with a turbo ion spray source and run in the positive ion mode. The turbo ion spray temperature was maintained at 350 °C, and a voltage of 5.0 kV was applied to the sprayer needle. N_2 was used as both turbo ion spray and nebulizer gas. The detection and quantification of CNO and clozapine were accomplished by multiple reactions monitoring the transitions m/z 343.1/192.1 for CNO and 327.2/270.0 for clozapine, respectively. MS/MS conditions were optimized automatically for each analyte, and the raw data were processed using Analyst Software (Applied Biosystems).

Islet Perifusion Experiments. Pancreatic islets were isolated as described (5). Islet perifusion experiments were carried out using a 12-channel Brandel suprafusion system (Brandel, Gaithersburg, MD). The housing, perifusion buffer, and chamber temperatures were kept at 37 °C. For each experiment (mouse), four parallel 200 μl perifusion chambers were loaded with 30 size-matched, hand-picked islets. Islets were perifused at 500 μl/min with Krebs-Ringer bicarbonate buffer (3 mM Ca^{2+}, 0.25% bovine serum albumin, 10 mM HEPES, equilibrated with 95% O_2/5% CO_2) containing either 2.8 mM or 16.7 mM glucose. CNO (final concentration: 0.1 μM) was added to the perifusion buffer supplying two out of the four chambers. Perfusates were collected from each chamber at regular intervals using a fraction collector. Insulin concentrations in the perfusates were determined via an ELISA kit (Crystal Chem Inc., Downers Grove, IL).

Static Islet Insulin Secretion Assay. Pancreatic islets were isolated from β-R-q Tg mice, and static islet insulin secretion assays were carried out as described (5). Batches of 10 islets were incubated in 12-well cell culture plates for 1 hr in a CO_2 incubator at 37 °C in the presence or absence of 0.1 μM CNO (glucose concentrations: 3.3 mM and 16.7 mM). The amount of insulin secreted during the incubation period was normalized to the total insulin content of each well (islets plus medium). Insulin concentrations were determined as described above.

References

1. Armbruster BN, Li X, Pausch MH, Herlitze S, Roth BL (2007) Evolving the lock to fit the key to create a family of G protein-coupled receptors potently activated by an inert ligand. Proc Natl Acad Sci USA 104:5163-5168.
2. Schöneberg T, Liu J, Wess J (1995) Plasma membrane localization and functional rescue of truncated forms of a G protein-coupled receptor. J Biol Chem 270:18000-18006.
3. Yarden Y, et al. (1986) The avian β-adrenergic receptor: primary structure and membrane topology. Proc Natl Acad Sci USA 83: 6795-6799.
4. Vasavada RC, et al. (1996) Overexpression of parathyroid hormone-related protein in the pancreatic islets of transgenic mice causes islet hyperplasia, hyperinsulinemia, and hypoglycemia. J Biol Chem 271:1200-1208.
5. Gautam D, et al. (2006) A critical role for β cell M_3 muscarinic acetylcholine receptors in regulating insulin release and blood glucose homeostasis in vivo. Cell Metab 3:449-461.
6. Wang X, Seed, B (2003) A PCR primer bank for quantitative gene expression analysis. Nucleic Acids Res 31:e154.

SI Figure legends

SI Fig. 1. Functional properties of the R-q and R-s mutant receptors studied in transfected mammalian cells. (*A-D*) Inositol phosphate (IP) accumulation assays. The ability of CNO (*A, B*) and ACh (*C, D*) to induce increases in intracellular inositol monophosphate (IP_1) levels was studied in COS-7 cells transiently expressing the WT mouse M3R (M3R) or the R-q and R-s mutant receptors. (*E-H*) cAMP accumulation assays. The ability of CNO (*E, F*) and ACh (*G, H*) to stimulate increases in intracellular cAMP levels was examined in COS-7 cells transiently expressing the WT mouse M3R (M3R) or the R-q and R-s mutant receptors. (*I*) Summary of maximum responses (E_{max} values) obtained in IP assays using COS-7 cells transfected with the indicated receptor constructs or vector DNA (pcD-PS). 'Basal' refers to IP_1 levels obtained with cells that had not been treated with CNO or ACh. (*J*) Summary of maximum responses (E_{max} values) obtained in cAMP assays using COS-7 cells transfected with the indicated receptor constructs (R-s; β1-AR, turkey β_1-adrenergic receptor; V2R, human V_2 vasopressin receptor) or vector DNA (pcD-PS). 'Basal' refers to cAMP levels measured in transfected cells that had not been treated with ligands. In each case, at least three independent concentration-response curves were obtained. Representative curves are shown in (*A-H*). Data are presented as means ± SEM in (*I*) and (*J*) (***$P < 0.0005$). ISO, isoproterenol; AVP, arginine vasopressin.

SI Fig. 2. Effect of CNO and ACh on intracellular calcium levels in receptor-expressing COS-7 cells. The WT mM3R and the R-q and R-s mutant receptors were transiently expressed in COS-7 cells. (*A-D*) Transfected cells were incubated with increasing concentrations of CNO (*A, B*) or ACh (*C, D*). Ligand-dependent increases in intracellular calcium levels were determined via FLIPR, as described in detail under SI Materials and Methods. Representative concentration-response curves, carried out in quadruplicate, are shown. Three independent experiments gave similar results. The CNO EC_{50} value at R-q was 87.3 ± 7.5 nM, and the ACh EC_{50} value at the WT mM3R was 1.3 ± 0.4 nM (means ± SEM; n = 3). RFU, relative fluorescence units.

SI Fig. 3. RT-PCR Analysis indicating islet selectivity of transgene expression in β-R-q and β-R-s Tg mice. (*A*) R-q and (*B*) R-s-specific PCR primer pairs were used to amplify cDNA prepared from the indicated tissues of adult β-R-q Tg and β-R-s Tg mice, respectively. Transgene expression was readily detectable in islets derived from both mouse lines, but was undetectable in other peripheral (liver, white adipose tissue (WAT), skeletal muscle (gastrocnemius muscle)) and central tissues (cerebral cortex, hypothalamus). Control samples that had not been treated with reverse transcriptase (RT) did not give any detectable RT-PCR products, confirming the absence of contaminating genomic DNA. GAPDH cDNA was amplified in all samples as an internal control. Amplicon sizes (in bp) were: R-q, 303; R-s, 308; GAPDH, 242.

SI Fig. 4. Physiological studies with β-R-q and β-R-s Tg mice in the absence of CNO. (*A, B*) Time course of body weight and blood glucose levels of freely fed β-R-q Tg mice and WT littermates. (*C, D*) Time course of body weight and blood glucose levels of freely fed β-R-s Tg and WT control mice. (*E*) Insulin tolerance test. Blood glucose levels were measured at the indicated time points following i.p. administration of insulin (0.75 U/kg; 4-5 month-old females). (*F-H*) Blood glucose, plasma insulin, and plasma glucagon levels of freely fed β-R-q and β-R-s Tg mice and WT control mice (3-month-old females). The data obtained with the two WT groups were pooled for the sake of clarity (no significant differences were found between these two groups). (*I, J*) Blood glucose and plasma insulin levels of fasted (10-12 hr) β-R-q and β-R-s Tg mice and control littermates (3-month-old females). Data are presented as means ± SEM (n = 5-8 per group). ***$P < 0.005$, as compared to the corresponding WT value.

SI Fig. 5. Effect of CNO on plasma insulin levels in β-R-q and β-R-s Tg mice. (*A, B*) CNO effects on plasma insulin levels in β-R-q and β-R-s Tg mice. β-R-q Tg (*A*) and β-R-s Tg mice (*B*) received a single i.p injection of increasing doses of CNO or vehicle (saline), and plasma insulin levels were measured at the indicated time points. Data are expressed as % increase in plasma insulin levels (pre-injection values were set equal to 100% in each individual mouse). Absolute basal insulin levels (prior to injection of saline or CNO) were (in ng/ml): β-R-q, 1.89 ± 0.34 (n = 24); β-R-s, 1.71 ± 0.30 (n = 20). Experiments were

carried out with 3-4-month-old female mice that had free access to food (4-6 mice per dose and/or group). Data presented as means ± SEM.

SI Fig. 6. CNO and clozapine plasma levels following CNO administration to WT mice. WT C57BL/6NTac mice (3-month-old females) received a single injection of CNO (1 mg/kg i.p.), and CNO and clozapine plasma levels were monitored for 2 hr by using LC-MS/MS (see SI Materials and Methods for details). Data are presented as means ± SEM (n = 3).

SI Fig. 7. CNO treatment of islets from β-R-q Tg mice enhances first- and second-phase insulin release in a glucose-dependent fashion. (*A*) Stimulatory effect of CNO on insulin release from perifused islets of β-R-q Tg mice. Islets were first perifused for 20 min at 2.8 mM glucose, either in the absence or presence of CNO (0.1 μM). After this period, the glucose concentration was raised to 16.7 mM, and islets were perifused either in the absence or presence of CNO (0.1 μM). For each individual experiment, islets from a single mouse were used (see SI Materials and Methods for experimental details). (*B*) First-phase insulin release at 16.7 mM glucose (defined as insulin release from 20-23 min expressed as area under the curve; AUC). (*B*) Second-phase insulin release at 16.7 mM glucose (defined as insulin release from 23-45 min expressed as AUC). Note that CNO showed a trend to increase insulin secretion even at 2.8 mM glucose. However, this CNO effect was not consistently observed in all experiments. Data are presented as means ± SEM of four independent experiments (6-8-month-old female mice). $*P < 0.05$, $**P < 0.005$, as compared to the corresponding non-CNO-treated β-R-q islets.

SI Fig. 8. CNO treatment of islets from β-R-s Tg mice enhances first- and second-phase insulin release in a glucose-dependent fashion. (*A*) Stimulatory effect of CNO on insulin release from perifused islets of β-R-s Tg mice. Islets were first perifused for 20 min at 2.8 mM glucose, either in the absence or presence of CNO (0.1 μM). After this period, the glucose concentration was raised to 16.7 mM, and islets were perifused either in the absence or presence of CNO (0.1 μM). For each individual experiment, islets from a single mouse were used (see SI Materials and Methods for experimental details). (*B*) First-

phase insulin release at 16.7 mM glucose (defined as insulin release from 20-23 min expressed as area under the curve; AUC). (*B*) Second-phase insulin release at 16.7 mM glucose (defined as insulin release from 23-45 min expressed as AUC). Data are presented as means ± SEM of three independent experiments (6-8-month-old female mice). $*P < 0.05$, $**P < 0.005$, as compared to the corresponding non-CNO-treated β-R-s islets.

SI Fig. 9. Effect of CNO on β-R-q Tg islets in a static insulin secretion assay. Isolated pancreatic islets prepared from 18-week-old male β-R-q Tg mice were incubated for 1 hr at 37 ^{o}C in Krebs solution containing the indicated glucose concentrations, either in the absence or presence of CNO (0.1 μM). The amount of insulin secreted into the medium during the 1 hr incubation period was normalized to the total insulin content of each well (islets plus medium). Data from a representative experiment are shown. Two additional experiments gave similar results.

SI Fig. 10. Physiological analysis of β-R-q and β-R-s Tg mice maintained on a high-fat diet. (*A, C*) Age-dependent increases in body weight in β-R-q (*A*) and β-R-s Tg (*C*) mice and control littermates. Mice were maintained either on regular chow (RC) or consumed a high-fat diet (HFD) for 12 weeks, starting from postnatal week 4. (*B, D*) Plasma insulin levels. Plasma insulin levels were measured in freely fed β-R-q (*B*) and β-R-s Tg (*D*) mice and control littermates maintained on a HFD. (*E*) Insulin tolerance test in HFD mice. Blood glucose levels were measured at the indicated time points following i.p. administration of insulin (0.75 U/kg). The data obtained with the two WT groups were pooled for the sake of clarity (no significant differences were found between these two groups). (*F, I*) I.p. glucose tolerance test in β-R-q (*F*) and β-R-s (*I*) Tg mice and control littermates maintained on a HFD. Blood glucose levels were measured at the indicated time points following i.p. administration of glucose (2 g/kg). Glucose was injected either alone (- CNO) or together with CNO (1 mg/kg i.p). (*G, H, J, K*) Plasma insulin levels in glucose-injected β-R-q (*G, H*) and β-R-s (*J, K*) Tg mice and control littermates maintained on a HFD. Plasma insulin levels were measured at the indicated time points following an i.p. glucose challenge (2 g/kg). Glucose was administered either alone or together with CNO (1 mg/kg i.p). In (*H*) and (*K*), total insulin secretion from 0-120 min is expressed as

area under the curve (AUC). Data are presented as means ± SEM (n = 8-12 male mice per group). *$P < 0.05$; **$P < 0.005$; ***$P < 0.0005$. In panels (*F*) and (*I*), responses between CNO-treated and non-CNO-treated Tg mice are compared (asterisks). In addition, responses between non-CNO-treated β-R-s Tg and WT mice are compared in panel (*I*) ($^{\#\#}P < 0.05$).

SI Fig. 11. Images of pancreatic sections from β-R-q and β-R-s Tg mice and WT littermates. β-R-q and β-R-s Tg mice and control littermates were treated for two weeks with daily injections of CNO (1 mg/kg i.p.) or saline (controls), as described under Materials and Methods. Representative pancreatic sections stained with an anti-insulin antibody are shown.

SI Fig. 12. Gene expression analysis using islets derived from β-R-q and β-R-s Tg mice and WT littermates. Islet gene expression was studied by real-time qRT-PCR using total RNA prepared from islets of β-R-q and β-R-s Tg mice and WT littermates. Prior to the isolation of total RNA, freshly prepared islets were cultured for 3 hr in 5.5 mM glucose in the presence or absence of 1 μM CNO. Data from three or four independent experiments using different sets of mice (~6-month-old males) were normalized relative to the expression of cyclophilin A (internal control). Results are presented as fold change in gene expression in CNO-treated versus untreated islets. Glut-2, glucose transporter 2; IRS-2, insulin receptor substrate 2; ACC2, Acetyl-CoA carboxylase-2. Data are shown as means ± SD (n = 3 or 4). *$P < 0.05$, **$P < 0.005$.

Table S1. Comparison of the ligand binding properties of the WT mM3R and the R-q and R-s mutant receptors

Receptor	[^{3}H]NMS binding		CNO binding	ACh binding
	K_d (pM)	B_{max} (nmol/mg)	K_i (μM)	K_i (μM)
WT mM3R	70.8 ± 9.8	9.05 ± 2.83	15.3 ± 2.1	4.91 ± 1.80
R-q	3,220 ± 760	5.65 ± 1.74	0.91 ± 0.12	ND[a]
R-s	2,820 ± 430	4.27 ± 1.63	0.15 ± 0.02	ND[a]

The WT mouse M3R (mM3R) and the R-q and R-s mutant receptors were transiently expressed in COS-7 cells. B_{max} and K_D values for [^{3}H]-NMS were determined from saturation binding experiments using membrane homogenates prepared from transfected COS-7 cells. CNO and ACh binding affinities (K_i) were determined in [^{3}H]-NMS competition binding assays (see Materials and Methods for details). Data are presented as means ± SEM of at least three independent experiments, each performed in duplicate.

[a]ND, no detectable inhibition of [^{3}H]NMS binding (20 nM) at ACh concentrations up to 0.1 mM.

Table S2. PCR primers used for qRT-PCR experiments

Mouse gene[a]	Primer sequence	Amplicon (bp)
Slc2a2 (Glut-2)	Forward: 5'CATTCTTTGGTGGGTGGC Reverse: 5'CCTGAGTGTGTTTGGAGCG	221
Gck (Glucokinase)	Forward: 5'AGGAGGCCAGTGTAAAGATGT Reverse: 5'CTCCCAGGTCTAAGGAGAGAAA	90
Ins2 (Insulin 2)	Forward: 5'-CTGGCCCTGCTCTTCCTCTGG Reverse: 5'-CTGAAGGTCACCTGCTCCCGG	204
Pcsk1[b]	Forward: 5' CTTTCGCCTTCTTTTGCGTTT Reverse: 5' TCCGCCGCCCATTCATTAAC	79
Pcsk2[c]	Forward: 5' AGAGAGACCCCAGGATAAAGATG Reverse: 5' CTTGCCCAGTGTTGAACAGGT	144
Irs2	Forward: 5' CTGCGTCCTCTCCCAAAGTG Reverse: 5' GGGGTCATGGGCATGTAGC	124
Acacb (ACC2)	Forward: 5' CGCTCACCAACAGTAAGGTGG Reverse: 5' GCTTGGCAGGGAGTTCCTC	161
Pcx[d]	Forward: 5' CTGAAGTTCCAAACAGTTCGAGG Reverse: 5' CGCACGAAACACTCGGATG	162
Pdx1	Forward: 5' CCCCAGTTTACAAGCTCGCT Reverse: 5' CTCGGTTCCATTCGGGAAAGG	177
Neurog3	Forward: 5' AGTGCTCAGTTCCAATTCCAC Reverse: 5' CGGCTTCTTCGCTTTTTGCTG	168
Nkx6-1	Forward: 5' CTGCACAGTATGGCCGAGATG Reverse: 5' CCGGGTTATGTGAGCCCAA	136
Neurod1	Forward: 5' ATGACCAAATCATACAGCGAGAG Reverse: 5' TCTGCCTCGTGTTCCTCGT	110
Mafa	Forward: 5' AGGAGGAGGTCATCCGACTG Reverse: 5' CTTCTCGCTCTCCAGAATGTG	113

Hnf4a	Forward: 5' CACGCGGAGGTCAAGCTAC Reverse: 5' CCCAGAGATGGGAGAGGTGAT	100
Ccnd1 (Cyclin D1)	Forward: 5' GCGTACCCTGACACCAATCTC Reverse: 5' CTCCTCTTCGCACTTCTGCTC	183
Ccnd2 (Cyclin D1)	Forward: 5' GAGTGGGAACTGGTAGTGTTG Reverse: 5' CGCACAGAGCGATGAAGGT	154
Cdk4	Forward: 5' ATGGCTGCCACTCGATATGAA Reverse: 5' TCCTCCATTAGGAACTCTCACAC	129
Myc	Forward: 5' ATGCCCCTCAACGTGAACTTC Reverse: 5' CGCAACATAGGATGGAGAGCA	228

[a]NCBI official gene symbol (name)

[b]Proprotein convertase 1

[c]Proprotein convertase 2

[d]Pyruvate carboxylase

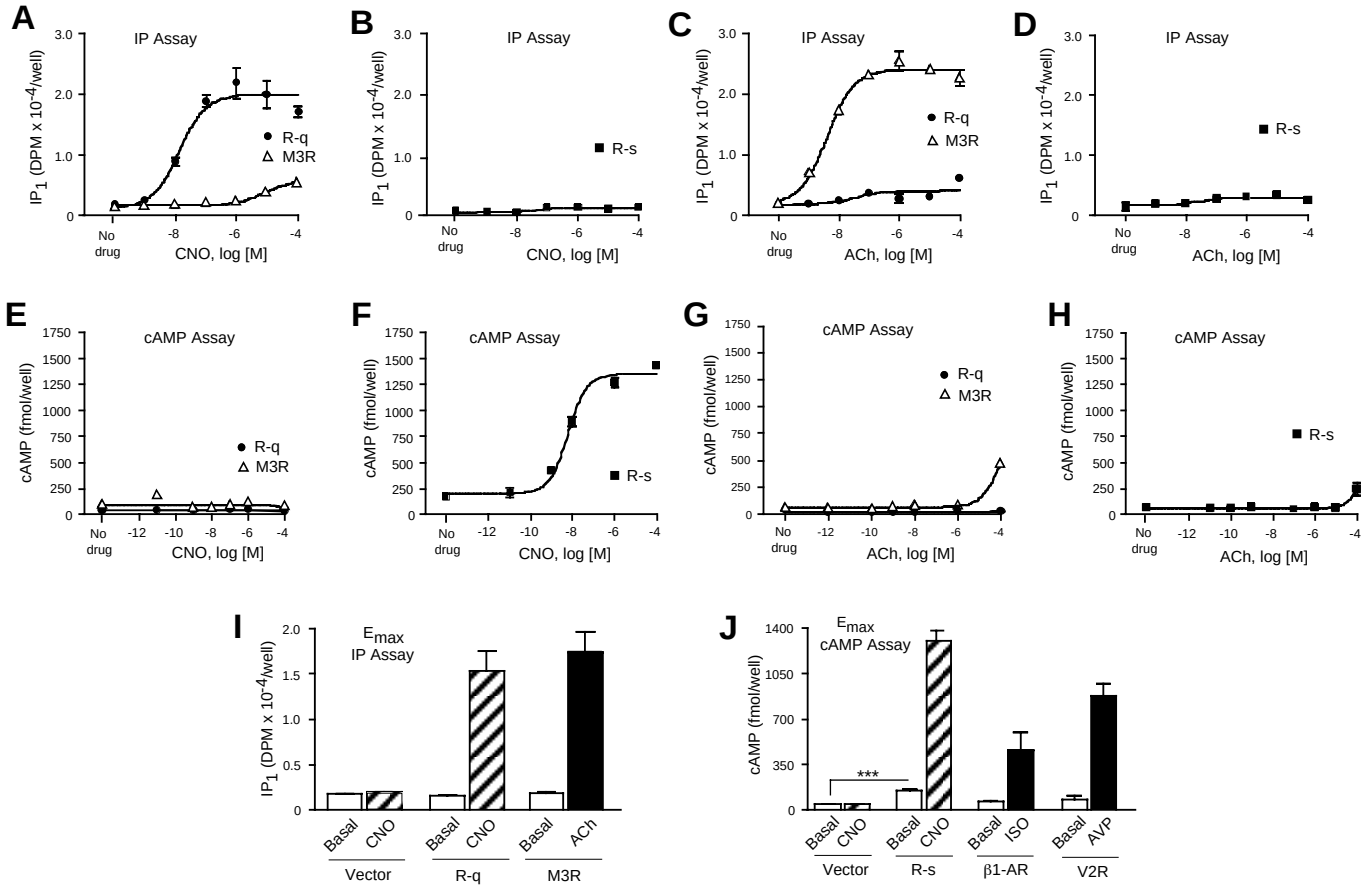
A
IP Assay
IP1 (DPM x 10-4/well)
R-q
M3R
No drug
CNO, log [M]
B
IP Assay
R-s
CNO, log [M]
C
IP Assay
R-q
M3R
ACh, log [M]
D
IP Assay
R-s
ACh, log [M]
E
cAMP Assay
cAMP (fmol/well)
R-q
M3R
CNO, log [M]
F
cAMP Assay
R-s
CNO, log [M]
G
cAMP Assay
R-q
M3R
ACh, log [M]
H
cAMP Assay
R-s
ACh, log [M]
I
Emax
IP Assay
Basal
CNO
ACh
Vector
R-q
M3R
J
Emax
cAMP Assay
***
ISO
AVP
Vector
R-s
β1-AR
V2R

SI Fig. 1

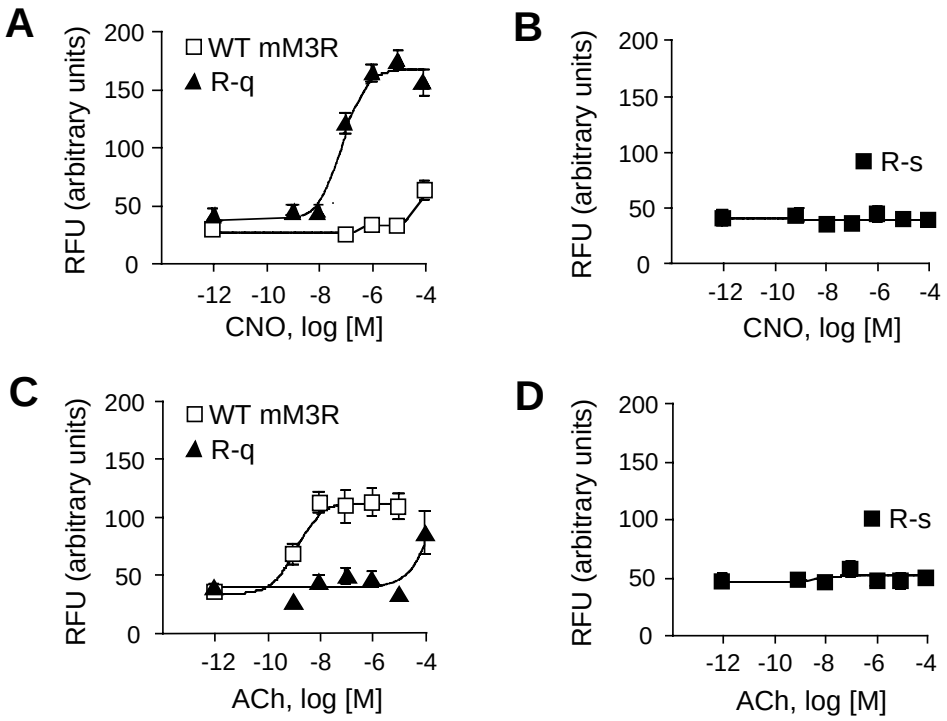
A
B
C
D
WT mM3R
R-q
R-s
RFU (arbitrary units)
CNO, log [M]
ACh, log [M]
200
150
100
50
0
-12
-10
-8
-6
-4

SI Fig. 2

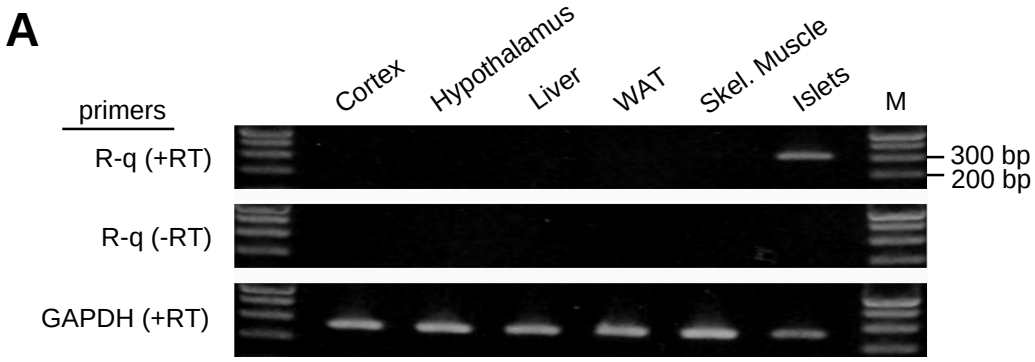

β-R-q mice

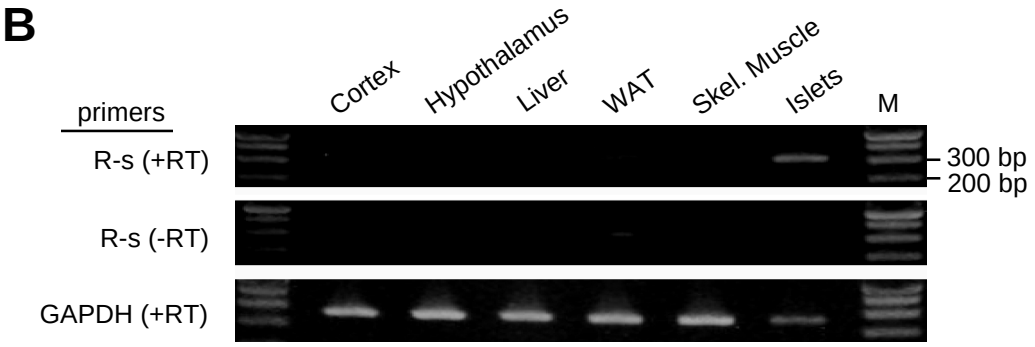

β-R-s mice

SI Fig. 3

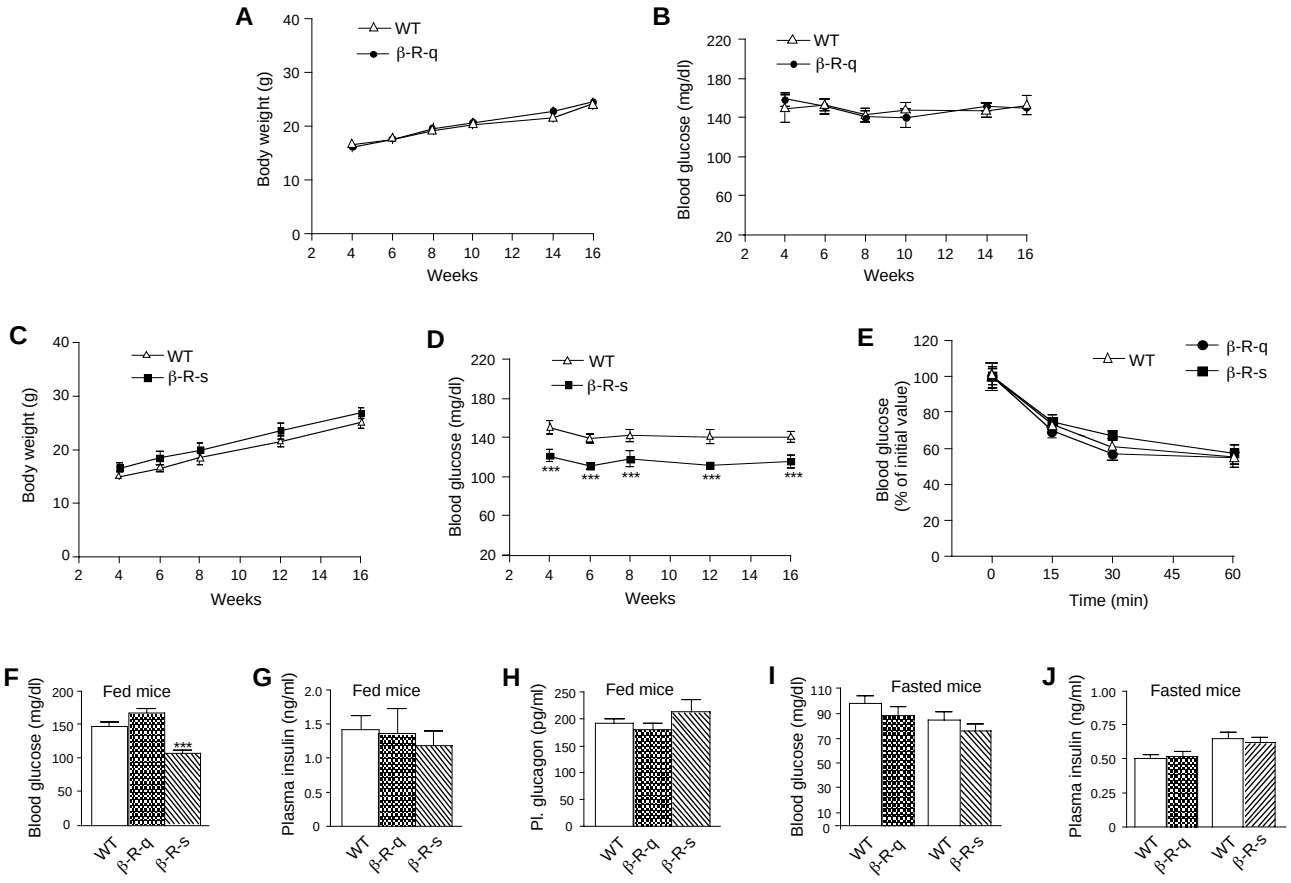
A
Body weight (g)
Weeks
WT
β-R-q
B
Blood glucose (mg/dl)
Weeks
WT
β-R-q
C
Body weight (g)
Weeks
WT
β-R-s
D
Blood glucose (mg/dl)
Weeks
WT
β-R-s
***
E
Blood glucose (% of initial value)
Time (min)
WT
β-R-q
β-R-s
F
Fed mice
Blood glucose (mg/dl)
***
WT
β-R-q
β-R-s
G
Fed mice
Plasma insulin (ng/ml)
WT
β-R-q
β-R-s
H
Fed mice
Pl. glucagon (pg/ml)
WT
β-R-q
β-R-s
I
Fasted mice
Blood glucose (mg/dl)
WT
β-R-q
WT
β-R-s
J
Fasted mice
Plasma insulin (ng/ml)
WT
β-R-q
WT
β-R-s

SI Fig. 4

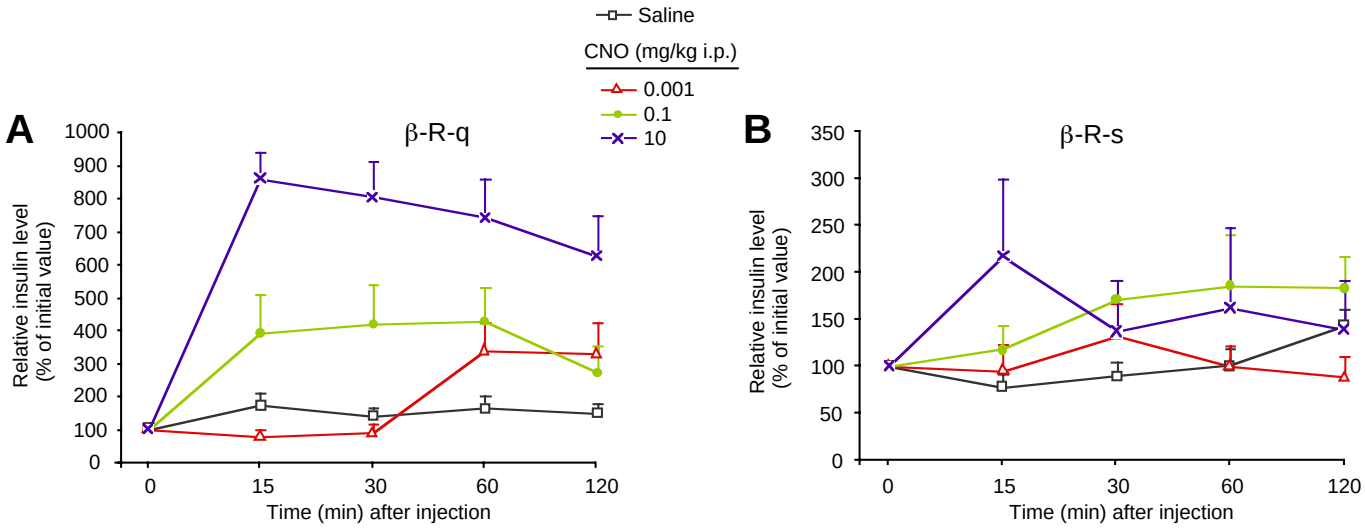
A
β-R-q
Saline
CNO (mg/kg i.p.)
0.001
0.1
10
Relative insulin level
(% of initial value)
1000
900
800
700
600
500
400
300
200
100
0
0
15
30
60
120
Time (min) after injection
B
β-R-s
Relative insulin level
(% of initial value)
350
300
250
200
150
100
50
0
0
15
30
60
120
Time (min) after injection

SI Fig. 5

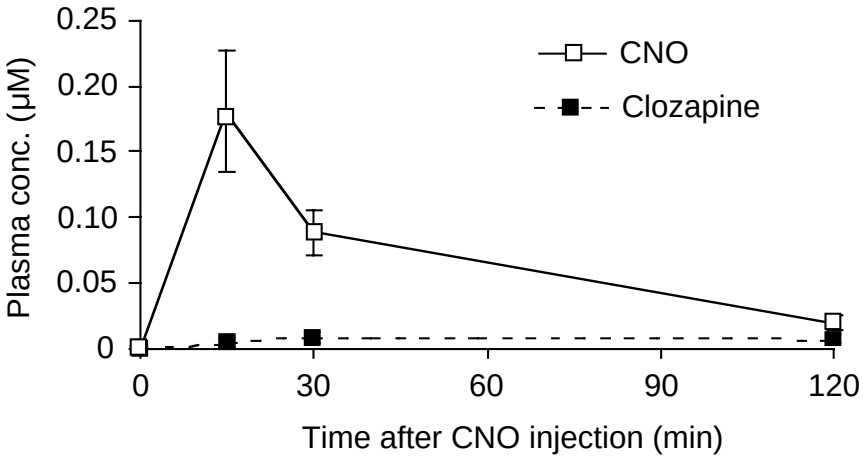
0.25
0.20
0.15
0.10
0.05
0
Plasma conc. (μM)
CNO
Clozapine
0
30
60
90
120
Time after CNO injection (min)

SI Fig. 6

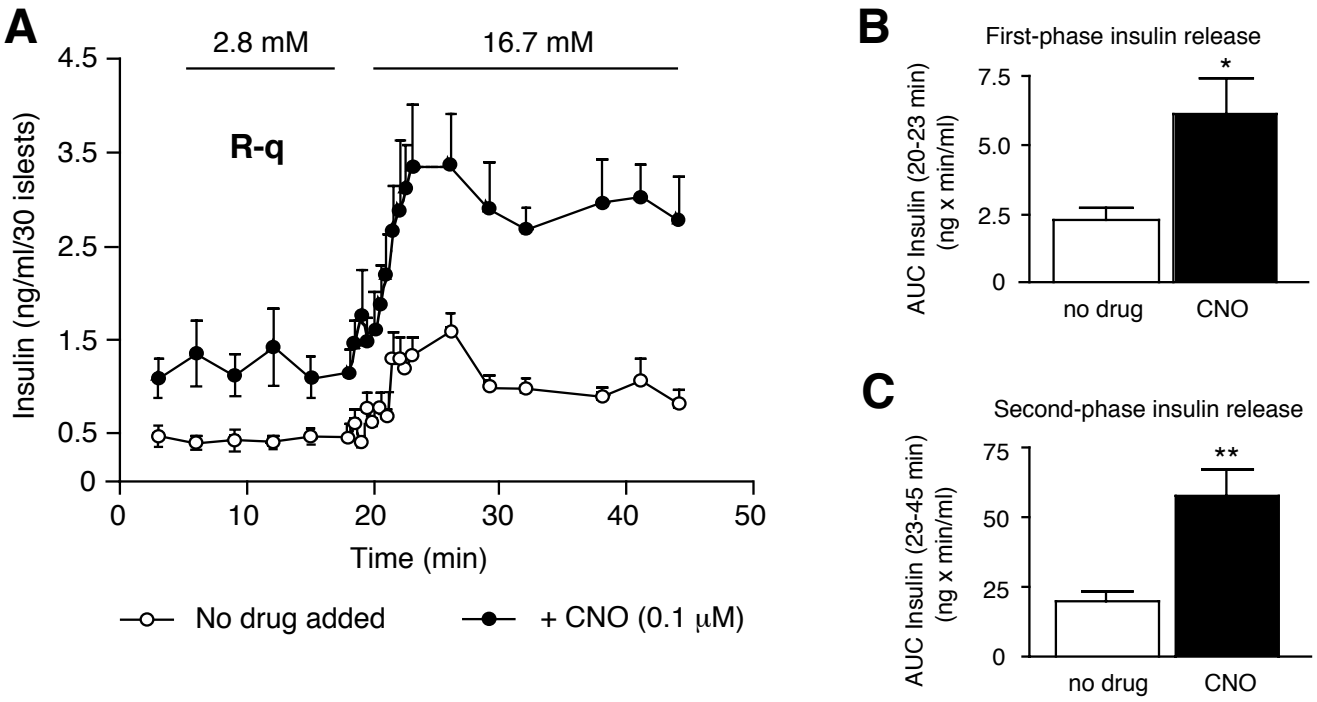
A
2.8 mM
16.7 mM
R-q
Insulin (ng/ml/30 islests)
4.5
3.5
2.5
1.5
0.5
0
0
10
20
30
40
50
Time (min)
No drug added
+ CNO (0.1 μM)
B
First-phase insulin release
AUC Insulin (20-23 min)
(ng x min/ml)
7.5
5.0
2.5
0
*
no drug
CNO
C
Second-phase insulin release
AUC Insulin (23-45 min)
(ng x min/ml)
75
50
25
0
**
no drug
CNO

SI Fig. 7

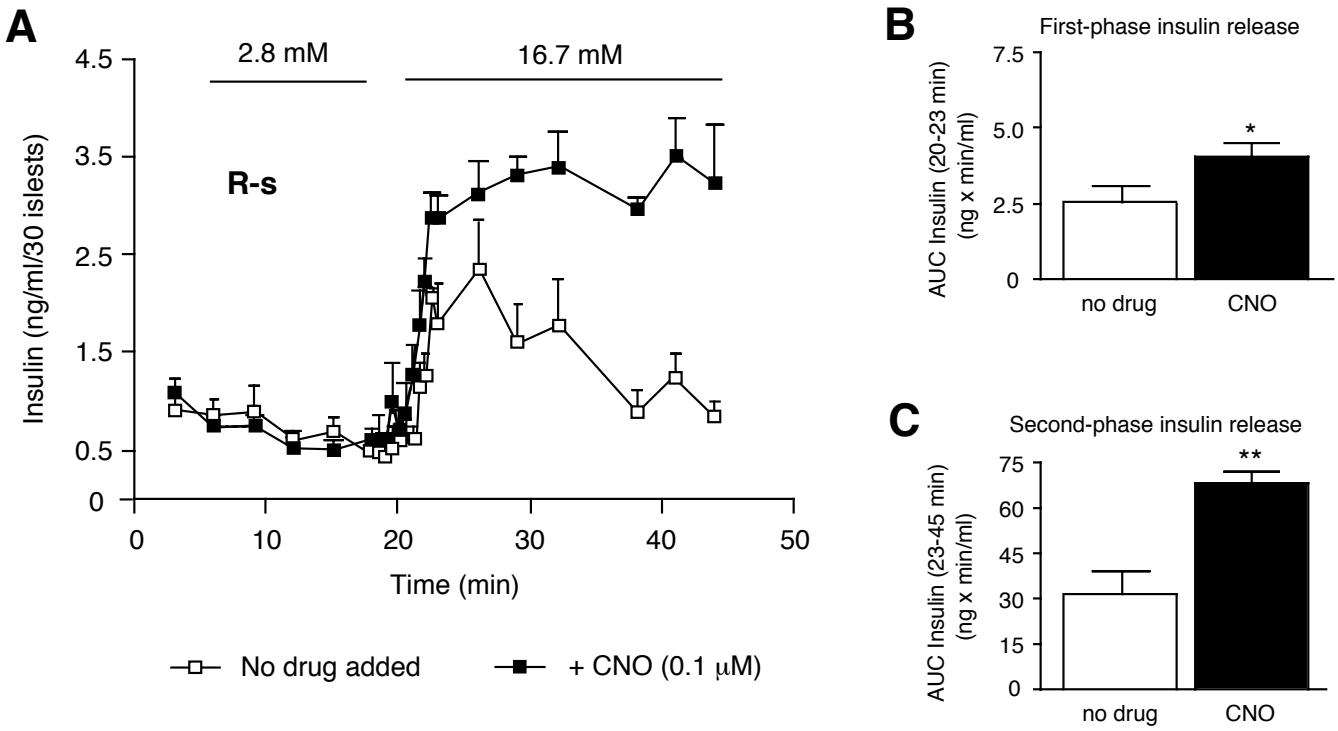
A
2.8 mM
16.7 mM
R-s
Insulin (ng/ml/30 islests)
4.5
3.5
2.5
1.5
0.5
0
0
10
20
30
40
50
Time (min)
No drug added
+ CNO (0.1 μM)
B
First-phase insulin release
AUC Insulin (20-23 min)
(ng x min/ml)
7.5
5.0
2.5
0
*
no drug
CNO
C
Second-phase insulin release
AUC Insulin (23-45 min)
(ng x min/ml)
75
60
45
30
15
0
**
no drug
CNO

SI Fig. 8

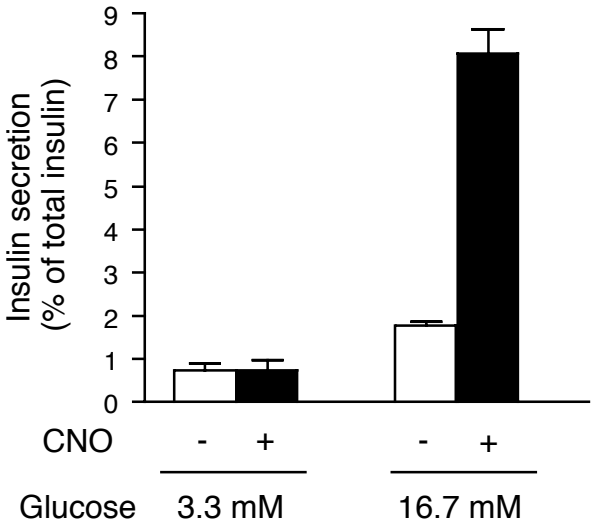
Insulin secretion
(% of total insulin)
9
8
7
6
5
4
3
2
1
0
CNO
-
+
-
+
Glucose
3.3 mM
16.7 mM

SI Fig. 9

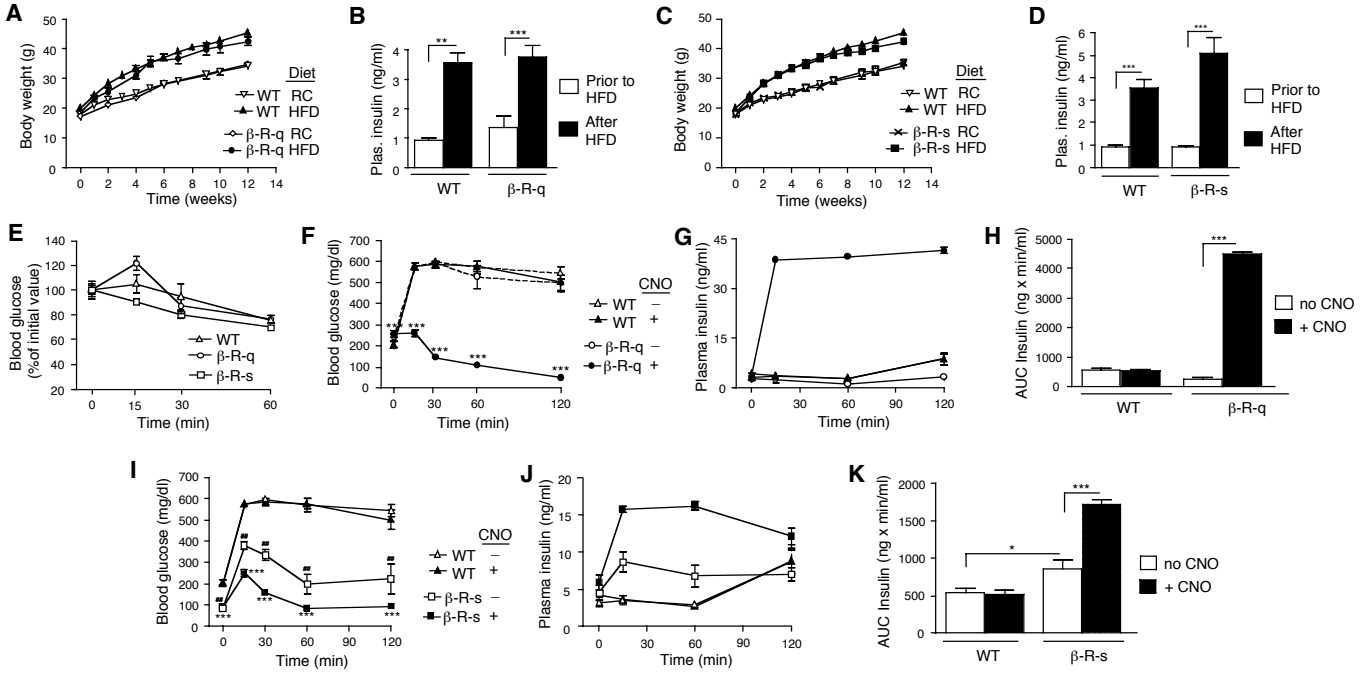
A
Body weight (g)
Time (weeks)
Diet
WT RC
WT HFD
β-R-q RC
β-R-q HFD
B
Plas. insulin (ng/ml)
Prior to HFD
After HFD
WT
β-R-q
C
Body weight (g)
Time (weeks)
Diet
WT RC
WT HFD
β-R-s RC
β-R-s HFD
D
Plas. insulin (ng/ml)
Prior to HFD
After HFD
WT
β-R-s
E
Blood glucose (%of initial value)
Time (min)
WT
β-R-q
β-R-s
F
Blood glucose (mg/dl)
Time (min)
CNO
WT –
WT +
β-R-q –
β-R-q +
G
Plasma insulin (ng/ml)
Time (min)
H
AUC Insulin (ng x min/ml)
no CNO
+ CNO
WT
β-R-q
I
Blood glucose (mg/dl)
Time (min)
CNO
WT –
WT +
β-R-s –
β-R-s +
J
Plasma insulin (ng/ml)
Time (min)
K
AUC Insulin (ng x min/ml)
no CNO
+ CNO
WT
β-R-s

SI Fig. 10

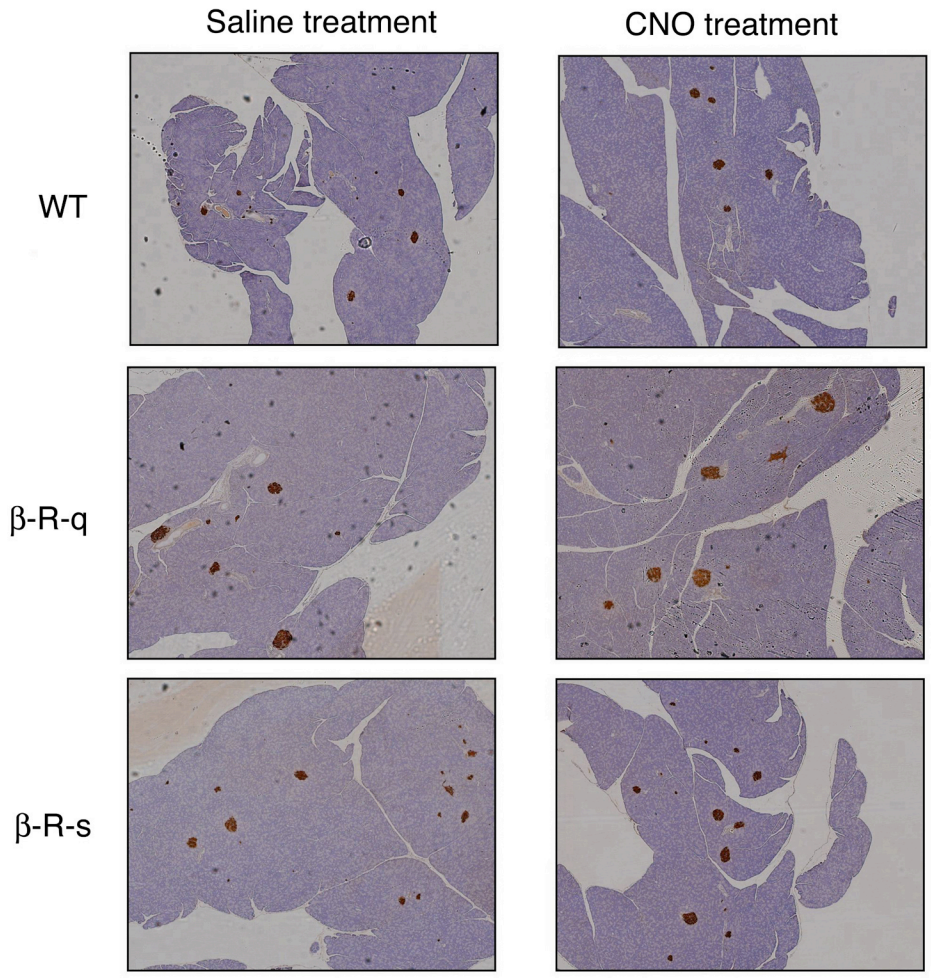

SI Fig. 11

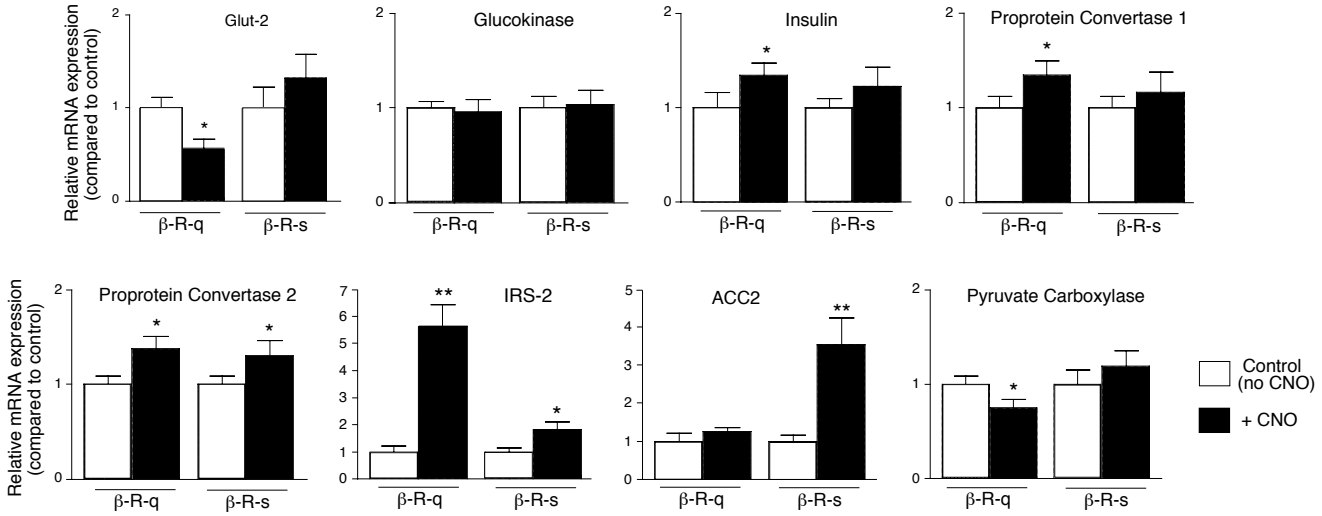
Relative mRNA expression (compared to control)
Glut-2
Glucokinase
Insulin
Proprotein Convertase 1
Proprotein Convertase 2
IRS-2
ACC2
Pyruvate Carboxylase
β-R-q
β-R-s
Control (no CNO)
+ CNO

SI Fig. 12